Published in final edited form as:
Conf Proc IEEE Eng Med Biol Soc. 2010 ; 2010: 2081–2084. doi:10.1109/IEMBS.2010.5626285.

Modeling the Effects of Deep Brain Stimulation on Sensorimotor Cortex in Normal and MPTP Conditions

S. Santaniello, IEEE [Member],
Institute of Computational Medicine, Johns Hopkins University, Baltimore, MD 21218 USA

J. T. Gale,
Department of Neurosciences, Cleveland Clinic, 44195 Cleveland, OH, USA (galej@ccf.org)

E. B. Montgomery Jr., and
Department of Neurology, University of Alabama at Birmingham, Birmingham, AL 35294 USA (emontgom@uab.edu)

S. V. Sarma, IEEE [Member]
Institute of Computational Medicine, Johns Hopkins University, Baltimore, MD 21218 USA

Abstract

Deep Brain Stimulation (DBS) is an effective surgical therapy for the treatment of movement disorders in Parkinson's disease (PD) and other neurological pathologies. DBS is known to modulate the spiking activity of the neurons within the basal ganglia, but how such modulation impacts the primary sensorimotor cortex is still uncertain. In this study a monkey was stimulated with DBS at several frequencies in the subthalamic nucleus (STN) before and after treatment with 1-methyl-4-phenyl-1,2,3,6-tetrahydropyridine (MPTP) to develop PD symptoms, while single unit recordings are simultaneously obtained from the sensorimotor cortex. We exploit such data to develop point-process input-output models of the cortical neurons. Our models describe the effects of stimulation in normal and MPTP conditions and investigate the influence of the stimulation frequency on the neuronal activity. Our models show increased synchronization of the cortical neurons in MPTP vs. normal conditions before stimulation, suggest that STN DBS impacts the cortical activity by antidromically eliciting spikes at the stimulation frequency, and support the hypothesis that high frequency DBS partially masks the effects of thalamo-cortical input.

I. Introduction

Deep Brain Stimulation (DBS) is an effective surgical therapy to treat movement disorders in Parkinson's disease (PD) [1], dystonia [2], and a growing number of other neurological pathologies [3]. It delivers high frequency (HF, i.e., >100 Hz) regular trains of current pulses within the basal ganglia, a set of subcortical nuclei involved in multiple segregated loops (e.g., limbic, prefrontal, oculomotor, motor, etc.) stemming from and returning to cortex [4]. Basal ganglia play a pivotal role in the motor loop, which has been hypothesized to affect the motor program selection and enabling of movement [3][4]. Along this motor loop (Fig.

corresponding author: S. V. Sarma; phone: +1-410-516-4381; fax: +1-410-516-5294; ssarma2@ jhu.edu.

1), basal ganglia receive convergent input from the motor and somatosensory cortex, relay this information through parallel pathways (e.g., direct and indirect pathway [4]), and finally project to the motor side of thalamus, which is believed to integrate and relay sensory information selectively to various cortical areas [5]. Studies on single unit [6][7][8][9] and local field potentials [10][11] from the basal ganglia-thalamic pathway in PD patients and non-human primates suggest that PD induces abnormal activity of the neurons in the basal ganglia (e.g., subthalamic nucleus (STN) [7][8], internal and external globus pallidus (GPi and GPe) [6]) and motor thalamus [9], elicits pathological synchronization within the nuclei [10][11], and decreases the neuronal selectivity to passive and voluntary movements [9]. It has been postulated that HF DBS modulates the neuronal spiking activity in GPi and thalamus [12][13], which in turn overrides pathological rhythms and entrains the target neurons to spike at the stimulation frequency [14]. Such effects positively correlate with improvements in motor symptoms [12][13].

It is still uncertain, however, how subcortical DBS finally impacts the cortex. Recently, [15] analyzed single unit recordings from primary motor (M1) cortex in a non human primate treated with MPTP during GPi DBS and reported that, during therapeutic stimulation (135 Hz), M1 neurons exhibited inhibitory phase locking to the stimulus, an overall decrease in mean discharge rate, and an increase in response specificity to passive limb movement. Dejean et al. [16], instead, reported that STN DBS induces antidromic cortical activation and reduces EEG slow-wave oscillations in awake cataleptic rats. Comparisons of normal vs. PD with and without DBS in the same species have not been made.

We investigate the spiking activity of sensorimotor cortex at rest (without DBS) and during STN DBS at different frequencies, both in normal and MPTP conditions, by exploiting single unit recordings from a non human primate. We develop point process models [17] to characterize the spiking propensity of cortical neurons as a function of the DBS input and the neurons' own spiking histories. Point process methods have been used to analyze the spike train activity for a broad range of neural systems [18] and were recently used to characterize the spiking activity in STN neurons from PD patients executing a directed-hand movement task [8][19]. As in [8], we use generalized linear methods (GLM) [20] to represent the point process conditional intensity function in terms of both short and long-term history dependence, thus capturing oscillations, bursting, and the impact of the stimulation frequency. Our models suggest that cortical neurons in MPTP conditions have increased synchronization and recurrent patterns that do not occur in normal conditions. They also show that each pulse of STN DBS induces antidromic activation, a rebound activity, and expires in less than 8 ms. Indications from the model parameters are also evident in traditional peristimulus time histograms (PSTHs) and cross-correlation histograms. Differently from such histograms, model parameters further characterize the relative impact of several concurrent input (e.g., DBS, ensemble activity, etc.) on the neuronal spiking propensity in different conditions and allow to detect multiple dynamical patterns simultaneously.

II. Methods

A. Data Collection

Recordings from a non-human primate were used in this study. Details about surgical procedures and data collection are in [21]. Briefly, the primate (macaca mulatta) was implanted with a recording chamber and received STN DBS via a reduced scale model of the human DBS lead. Microelectrode recordings were alternatively obtained from 7 sites in the sensorimotor cortex during DBS (Fig.1, positions later confirmed by histological examination). DBS consisted of constant current biphasic square pulses with the cathodic phase preceding the anodic phase (ventral contact). The pulse width was 90 μs per phase and the amplitude was 80% of the value that produced tonic contraction (presumed activation of internal capsule). DBS frequencies were 50, 100 and 130 Hz. Stimulation/recording sessions were made both before and after that the primate was treated with MPTP and developed a stable PD state with contralateral rigidity and bradykinesia. During each session, continuous recordings of neuronal activity were made 30 s before and 30 s during DBS. The animal was awake and quietly sitting. Extracellular signals were band-pass filtered, amplified, digitized (25 kHz), and sorted offline into individual unit activities (Q units per session, with Q ranging from 2 to 7, depending on position and session, Fig.1). For each unit, time stamps of the detected spikes were recorded [12] [21].

B. Point Process Modeling

We formulated point process models (PPMs) to relate the spiking propensity of neurons to their own spiking history, the history of other neurons simultaneously recorded (same ensemble), and DBS pattern. We used the model parameters to analyze the effects of DBS and synchronization [8].

A neural spike train is treated as a series of random binary events that occur continuously in time (point process), where the 1s are spike times and the 0s the times at which no spikes occur [17]. A PPM of a neural spike train is characterized on an observation interval (0, T] by defining the conditional intensity function (CIF)

$$\lambda(t|H_t)=\lim_{\Delta\to 0} P(N(t+\Delta)-N(t)=1|H_t)/\Delta \quad (1)$$

where $N(t)$ is the number of spikes in (0, t] for t in (0, T], H_t the history of spikes up to t, P the probability [17]. $\lambda(t|H_t)$ is a generalized history-dependent rate function and $\lambda(t|H_t)\Delta$ approximately gives the spiking propensity at t if Δ is small [17]. Because the CIF completely characterizes a spike train, defining a model for the CIF defines a model for the spike train [22]. For each neuron, we defined the GLM model:

$$\lambda(k|H_k)=e^{\alpha}\times\lambda_0(k|H_k)\times\lambda_S(k|H_k)\times\lambda_E(k|H_k) \quad (2)$$

where $\lambda_O(k|H_k)$ accounts for the neuron own spiking history, $\lambda_S(k|H_k)$ for DBS (if applied) and $\lambda_E(k|H_k)$ for dependencies from other neurons in the ensemble. k is the k-th bin (ms) and e^{α} accounts for history-independent activity. We defined:

$$log\lambda_0(k|H_k)=\sum_{r=1}^{10}\beta_r dN(k-r,k-r+1)+\sum_{r=11}^{18}\beta_r dN(k-5(r-8),k-5(r-9)) \quad (3)$$

$$log\lambda_S(k|H_k)=\sum_{\nu=1}^{8}\gamma_\nu dN_S(k-\nu,k-\nu+1) \quad (4)$$

$$log\lambda_E(k|H_k)=\sum_{q=1}^{Q}\left\{\sum_{h=1}^{10}\delta_{h,q}dN_q(k-h,k-h+1)+\sum_{h=11}^{18}\delta_{h,q}dN_q(k-5(h-8),k-5(h-9))\right\} \quad (5)$$

where $dN(a, b)$ and $dN_q(a, b)$ are the number of spikes fired by the given neuron or the q-th neuron in the ensemble in the interval $[a, b)$ (in ms), and $dN_S(a, b)$ is the number of DBS pulses delivered in the same interval. $\{\beta_r\}_{r=1}^{10}$ measure the effects of the spiking history in the previous 10 ms, thus detecting refractoriness and bursting. For example, if $e^{\beta 1} \approx 0$, then for any given time bin k, the probability to spike in that bin is close to 0 if the neuron had a spike in the previous ms bin (refractory period). As well, if $e^{\beta 5}$ is significantly larger than 1, then for any time bin k, the probability that the neuron spikes in that bin is modulated up if it had a spike 5 ms prior to k, suggesting bursting [8]. The $\{\beta_r\}_{r=11}^{18}$ parameters account for the history in the previous 10–50 ms and detect oscillations [8]. For example, if $e^{\beta 18}$ is significantly larger than 1, then the probability that the neuron will spike in bin k is modulated up if it spiked 45–50 ms prior to k, suggesting 20–22 Hz oscillations.

The $\{\delta_{h,q}\}_{h=1}^{18} q=1,\ldots,Q$ show dependencies on other cells. For example, if for a given value of q, $e^{\delta 5,q}$ is significantly larger than 1, then for any bin k, the probability that the neuron spikes is modulated up if the q-th neuron in its ensemble spiked 5 ms prior to k, suggesting phase-locked activity of the two cells. Similarly, $\{\gamma_\nu\}_{\nu=1}^{8}$ measure the dependency from the DBS input in the previous 8 ms.

For each neuron, both with and without DBS, an estimate of the parameter vector $\Theta=\left\{\alpha,\beta_r,\gamma_\nu,\{\delta_{h,q}\}_{q=1}^{Q}\right\}$ and 95% confidence bounds was provided by maximizing the likelihood of observing the recorded spike trains [8][17].

For each neuron, 80% of spike trains were for parameter estimation and 20% for validation. The set of history bins (a, b in $dN(a, b)$) in (3–5) was chosen by minimizing the Akaike's criterion [22]. The goodness-of-fit of each PPM was assessed on the validation data with the Kolmogorov-Smirnov (KS) plot after time rescaling of the spike trains [22]. We included in this study only neurons with an average spiking rate ≥5 Hz before stimulation and whose PPM had a KS plot within the 95% confidence bounds [8][22] (Table I).

III. Results

We compared PPMs estimated for neurons in normal and MPTP conditions, with and without DBS. Results are summarized in Fig.2–4 and Table II–IV (discharge frequency is reported in tables as mean±S.E.M. [12]).

A. MPTP vs. Normal with No DBS Input

Table II and Fig.2 compare results in MPTP vs. normal conditions at rest. MPTP neurons show refractoriness (Fig.2b), bursting with period of 3–7 ms, and 20–30 Hz oscillations, with the most recurrent inter-spike interval between 45 and 50 ms (8 out of 14 neurons). Parameters in MPTP vs. normal conditions significantly differed (unpaired t-test, p-value $p < 0.001$). Moreover, α is significantly higher in normal vs. MPTP conditions (Fig.2a,e), which accounts for the difference in the discharge frequency. Differences also arose in parameters $\delta_{h,q}$. Fig.2c,g show the $\delta_{h,q}$'s for a specific value of q in an MPTP and normal neuron: the spike propensity of the MPTP neuron increases if the q-th neuron in the ensemble has spiked in the previous 4–6 ms or 15–20 ms and suggests possible synchronization, also indicated by cross-correlation histogram (Fig.2d). The normal neuron (Fig.2g,h), instead, has milder dependency, with no significant peak in the $\delta_{h,q}$'s. Table II (last two rows) summarizes results for the population: we estimated 51 sets of $\delta_{h,q}$'s $h = 1, \ldots, 18$, for MPTP cells, 241 for normal cells (one for each couple of cells in the same ensemble) and reported the number of sets with significant dependencies in 3–7 and 10–30 ms. Our results suggest that normal spike trains in cortex tend to a Poisson-like distribution with mild mutual dependencies, while prominent bursts, oscillations and synchronization arise in MPTP conditions.

B. Effects of DBS Frequency on Normal Neurons

Table III and Fig.3 compare the effects of DBS at various frequencies in normal conditions. Normalized PSTHs (bin size 0.08 ms [3][12]) of two cells in Fig.3d,h indicate that DBS increases the probability of spiking 3 to 5 ms after the stimulus. The high temporal consistency of the neuronal response to the pulses suggests early antidromic activation [12], followed by a second spike (3–5 ms after pulse), a recovery period (5–7 ms after pulse), and eventually a third spike (7–8 ms after pulse). The impact of each pulse after 8 ms is not significant and may be neglected. PPMs confirm that and also suggest a few differences in the neuronal behavior: 100 Hz DBS elicits a phase-locked spiking activity in the cortical neuron (e^{α} strongly drops as soon as DBS is applied, $e^{\gamma\nu} > 10$ $\nu = 4, \ldots, 8$, Fig.3g), which overrides the dependency from the previous spiking history. 50 Hz DBS, instead, has milder impact (higher value of α, no significant difference from spike trains at rest, and lower γ_ν's, Fig.3c).

C. MPTP vs. Normal Conditions under 130 Hz DBS

Table IV and Fig.4 compare results in MPTP vs. normal conditions under 130 Hz DBS. HF DBS resulted in strong antidromic activation (<2ms since DBS pulse) but mild spiking 4–5 ms after the pulse. Such effects were noted both in normal and MPTP neurons and captured by the PPM parameters: 95% confidence bounds of $e^{\beta}r$ include 1 $\forall r$, $e^{\gamma 1} \gg 1$, $e^{\gamma\nu} \ll 1$ $\nu =$ 3,4 (strong post-stimulus inhibition), mild recovery occurs for $\nu = 5,6$ but no late spike (7–8 ms) is reported. No significant difference was noted in normal vs. MPTP cells, while the prominence of antidromic activation over secondary phenomena suggests that HF DBS may mask at cortical level the impact of the thalamo-cortical pathway.

IV. Conclusion

An extremely rare experimental set up and a point process modeling framework are used in this paper to investigate the dynamical behavior of neurons in the sensorimotor cortex in normal and MPTP conditions, measure the impact of STN DBS, and show the temporal dependencies between neurons in the same ensemble. Our models indicate increased synchronization in MPTP vs. normal conditions, suggest that DBS antidromically elicits spikes at the frequency of stimulation (which may temporally mask the effects of thalamo-cortical projections), and account for a different modulation of the cortical spike propensity in MPTP vs. normal conditions. Model parameters also quantify the relative impact of different factors (e.g., DBS, ensemble activity) on the neuronal spiking propensity.

References

1. Benabid AL, Chabardes S, Mitrofanis J, Pollak P. Deep brain stimulation of the subthalamic nucleus for the treatment of Parkinson's disease. Lancet Neurol. 2009 Jan.8:67–81. [PubMed: 19081516]
2. Ostrem JL, Starr PA. Treatment of dystonia with deep brain stimulation. Neurotherapeutics. 2008 Apr.5:320–330. [PubMed: 18394573]
3. Montgomery EB, Gale JT. Mechanisms of action of deep brain stimulation (DBS). Neurosci. Biobehav. Rev. 2008 Jun.32:388–407. [PubMed: 17706780]
4. DeLong MR, Wichmann T. Circuits and circuit disorders of the basal ganglia. Arch. Neurol. 2007 Jan.64:20–24. [PubMed: 17210805]
5. Haber SN, Calzavara R. The cortico-basal ganglia integrative network: the role of the thalamus. Brain Res. Bull. 2009 Feb.78:69–74. [PubMed: 18950692]
6. Raz A, Vaadia E, Bergman H. Firing patterns and correlations of spontaneous discharge of pallidal neurons in the normal and the tremulous 1-methyl-4-phenyl-1,2,3,6-tetrahydropyridine vervet model of parkinsonism. J. Neurosci. 2000 Nov.20:8559–8571. [PubMed: 11069964]
7. Gale JT, Shields DC, Jain FA, Amirnovin R, Eskandar EN. Subthalamic nucleus discharge patterns during movement in the normal monkey and Parkinsonian patient. Brain Res. 2009 Mar.1260:15–23. [PubMed: 19167367]
8. Sarma SV, Eden UT, Cheng ML, Williams ZM, Eskandar E, Brown EN, Hu R. Using point process models to compare neural spiking activity in the subthalamic nucleus of Parkinson's patients and a normal primate. IEEE Trans. Biomed. Eng. 2010 Jun.56:1297–1305. [PubMed: 20172804]
9. Pessiglione M, Guehl D, Rolland AS, François C, Hirsch EC, Féger J, Tremblay L. Thalamic neuronal activity in dopamine-depleted primates: evidence for a loss of functional segregation within basal ganglia circuits. J Neurosci. 2005 Feb.25:1523–1531. [PubMed: 15703406]
10. Brown P. Abnormal oscillatory synchronization in the motor system leads to impaired movement. Curr. Opin. Neurobiol. 2007 Dec.17:656–664. [PubMed: 18221864]
11. Kühn AA, Tsui A, Aziz T, Ray N, Brücke C, Kupsch A, Schneider GH, Brown P. Pathological synchronization in the subthalamic nucleus of patients with Parkinson's disease relates to both bradykinesia and rigidity. Exp Neurol. 2009 Feb.215:380–387. [PubMed: 19070616]
12. Montgomery EB. Effects of GPi stimulation on human thalamic neuronal activity. Clin. Neurophysiol. 2006 Dec.117:2691–2702. [PubMed: 17029953]
13. Hashimoto T, Elder CM, Okun MS, Patrick SK, Vitek JL. Stimulation of the subthalamic nucleus changes the firing pattern of pallidal neurons. J. Neurosci. 2003 Mar.23:1916–1923. [PubMed: 12629196]
14. Kuncel AM, Cooper SE, Wolgamuth BR, Grill WM. Amplitude- and frequency-dependent changes in neuronal regularity parallel changes in tremor With thalamic deep brain stimulation. IEEE Trans. Neural Syst. Rehabil. Eng. 2007 Jun.15:190–197. [PubMed: 17601188]
15. Johnson MD, Vitek JL, McIntyre CC. Pallidal stimulation that improves Parkinsonian motor symptoms also modulates neuronal firing patterns in primary motor cortex in the MPTP-treated monkey. Exp. Neurol. 2009 Sep.219:359–362. [PubMed: 19409895]

16. Dejean C, Hyland B, Arbuthnott G. Cortical effects of subthalamic stimulation correlate with behavioral recovery from dopamine antagonist induced akinesia. Cereb. Cortex. 2009 May. 19:1055–1063. [PubMed: 18787234]

17. Snyder, DL.; Miller, MI. Random Point Processes in Time and Space. New York, NY: Springer; 1991.

18. Truccolo W, Eden UT, Fellows MR, Donoghue JP, Brown EN. A point process framework for relating neural spiking activity to spiking history, neural ensemble, and extrinsic covariate effects. J Neurophysiol. 2005 Feb.93:1074–1089. [PubMed: 15356183]

19. Eden, UT.; Amirnovin, R.; Brown, EN.; Eskandar, EN. Proc. Joint Statistical Meetings. Salt Lake City (UT): 2007 Jul-Aug. Constructing models of the spiking activity of neurons in the subthalamic nucleus of Parkinson‘s patients.

20. McCullagh P, P.; Nelder, JA. Generalized Linear Models. 2nd ed.. Boca Raton, FL: CRC; 1990.

21. Gale, JT. Ph.D. thesis. Ohio: Kent State Univ.; 2004. Basis of periodic activities in the BG-thalamic-cortical system of the rhesus macaque.

22. Brown, EN.; Barbieri, R.; Eden, UT.; Frank, LM. Likelihood methods for neural data analysis. In: Feng, J., editor. Computational Neuroscience: A Comprehensive Approach. London, UK: CRC; 2003. p. 253-286.

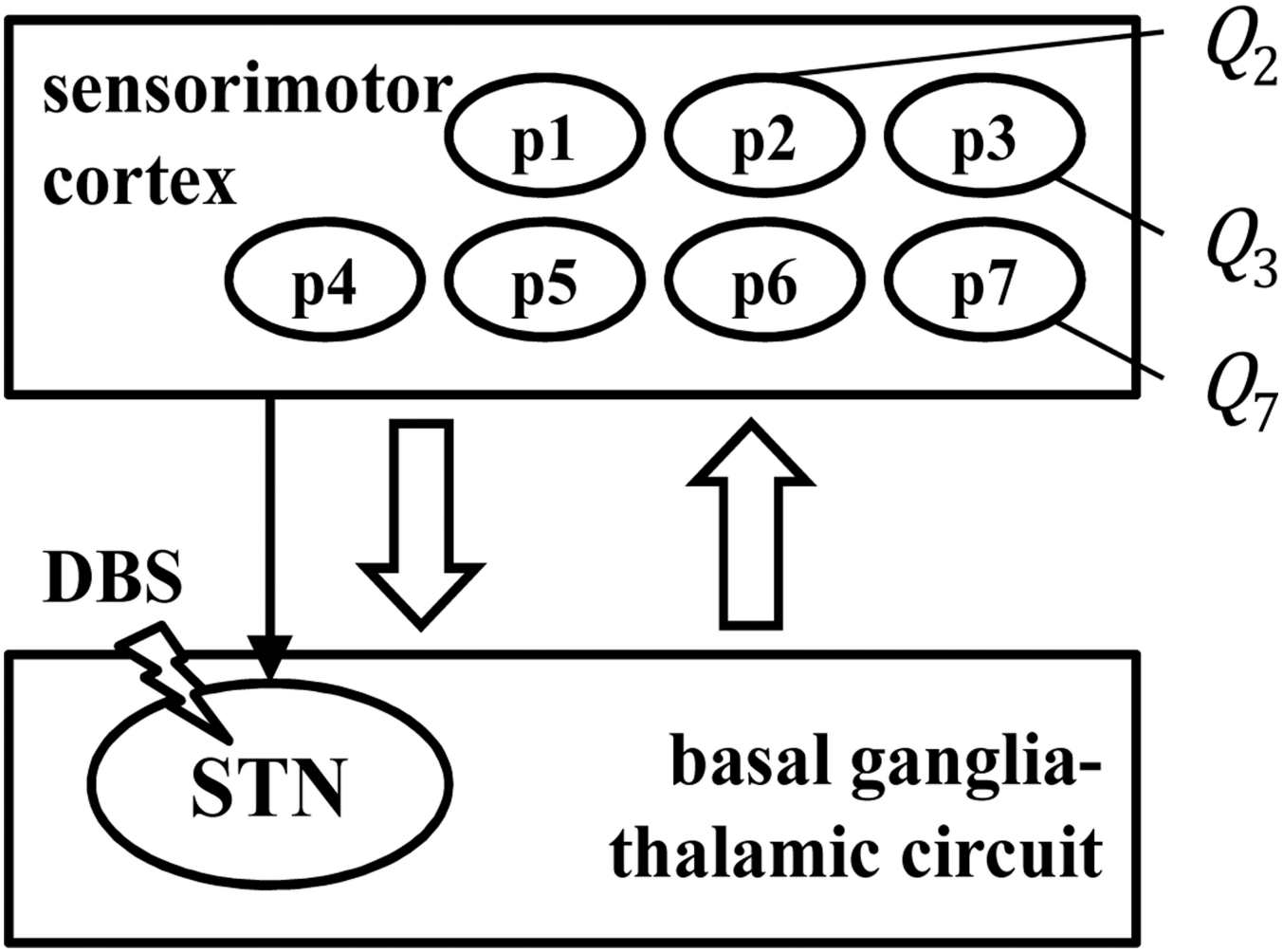

Fig. 1.

Cortico-basal ganglia-thalamo-cortical loop. There are several projections from sensorimotor cortex to the basal ganglia (in particular, to the STN). p1 … 7 qualitatively indicate different recording sites in this study, with Q_i neurons simultaneously recorded in *pi* $i = 1, \ldots 7$.

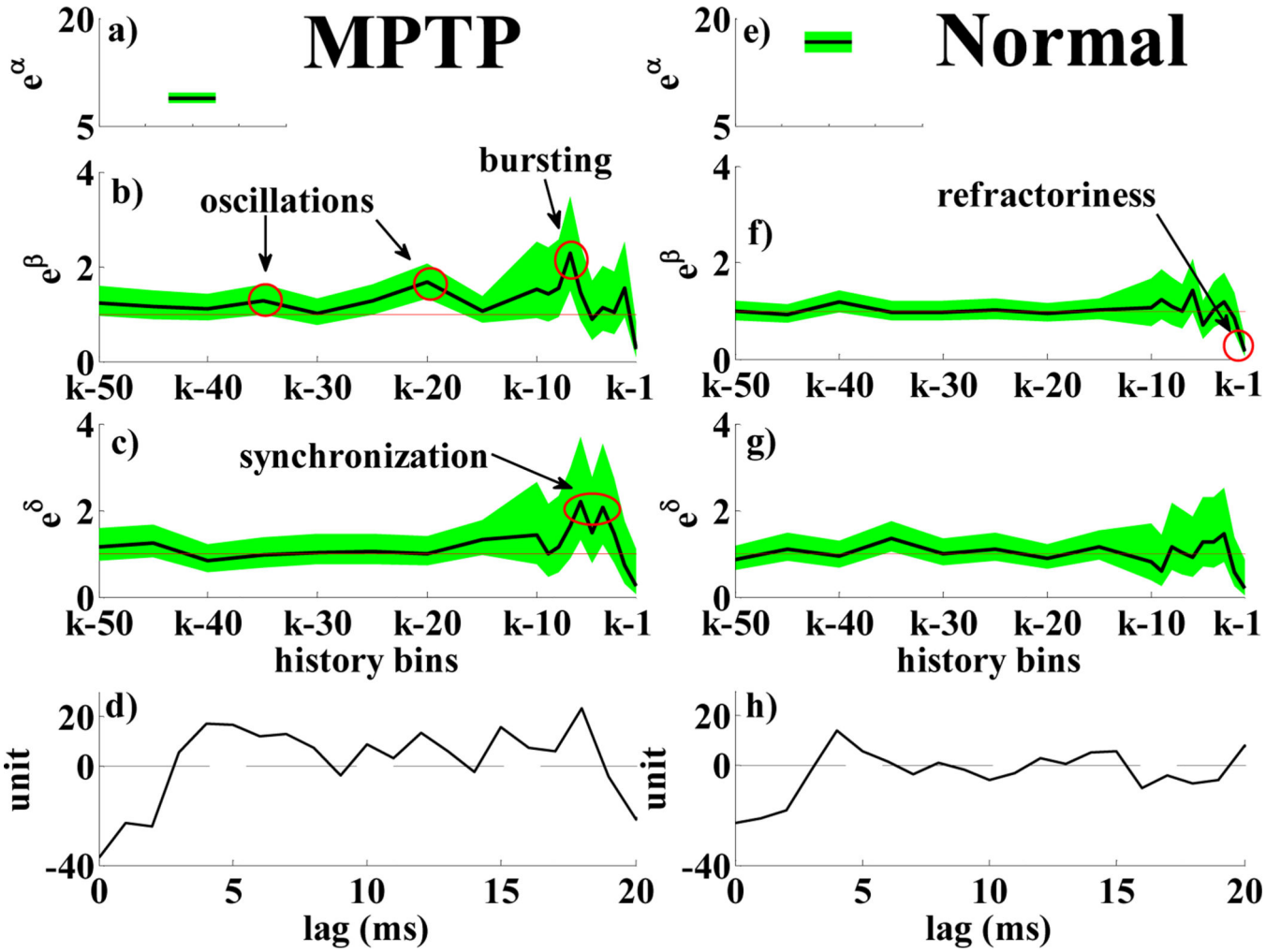

Fig. 2.

PPM for a MPTP (a–d) and a normal (e–h) neuron: a), e) e^{α}; b), f) $e^{\beta r}$, $r = 1, \ldots, 18$ vs. history bins for a generic time bin k; c), g) $e^{\delta h,q}$, $h = 1, \ldots, 18$ vs. history bins for a specific q and time bin k. d), h) mean-subtracted cross-correlation histogram of each neuron with the q-th one in its ensemble (lag: 50 ms, details in [7]) Parameters in a–c),e–g) are black lines, 95% confidence intervals are shaded green areas, $e^{0} = 1$ is a red line.

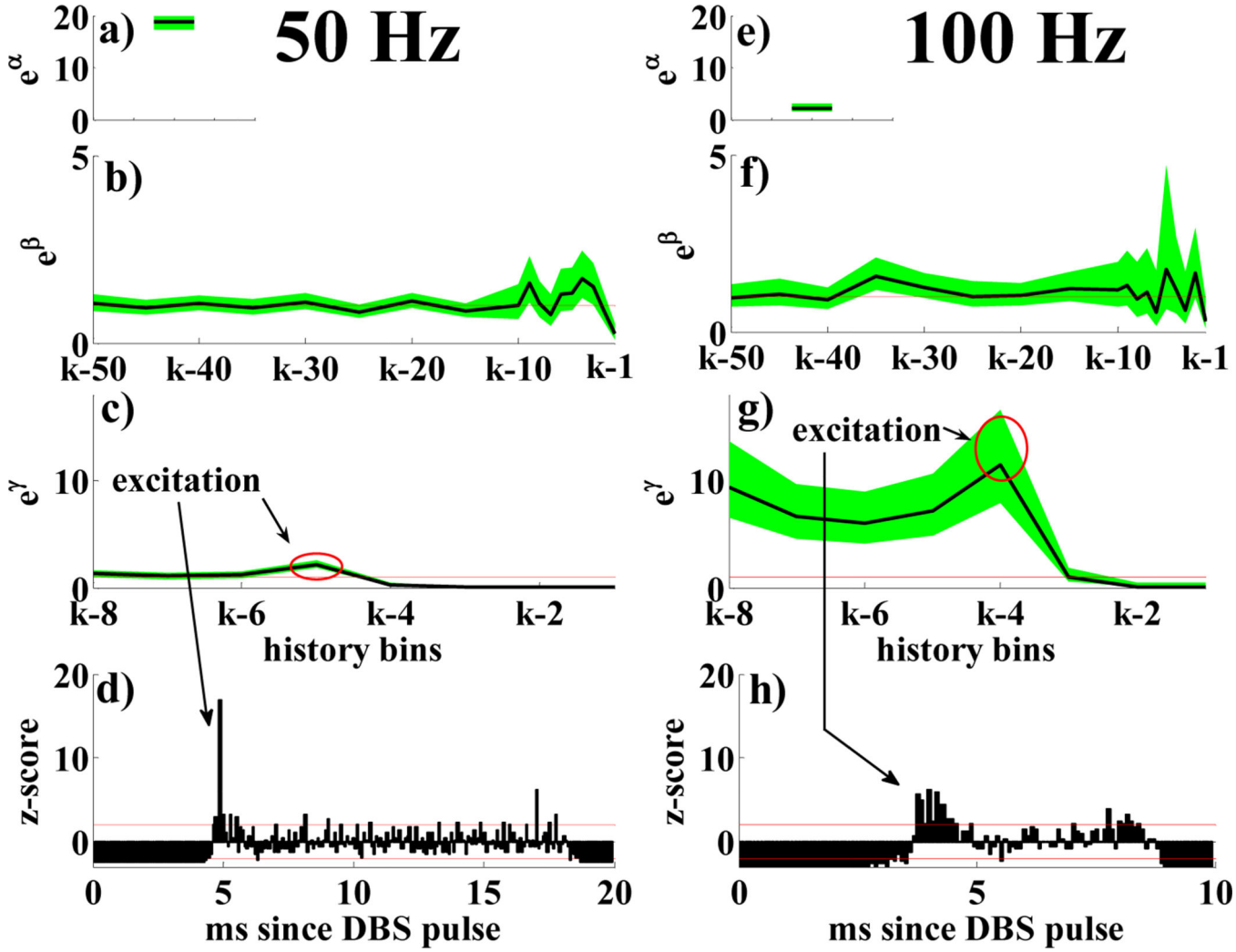

Fig. 3.

PPM for normal neurons with 50 (a–d) and 100 Hz (e–h) DBS: a), e) e^{α}; b), f) $e^{\beta r}$, $r = 1, \ldots, 18$ vs. history bins for a generic time bin k; c), g) $e^{\gamma \nu}$, $\nu = 1, \ldots, 8$ vs. history bins for a generic time bin k. d), h) PSTHs (normalization to z-score based on the prestimulation activity [12]). Histograms <−1.96 or >1.96 (red lines) mean significant inhibition or excitation respectively. Parameters in a–c),e–g) are black lines, 95% confidence intervals are shaded green areas, $e^{0} = 1$ is a red line.

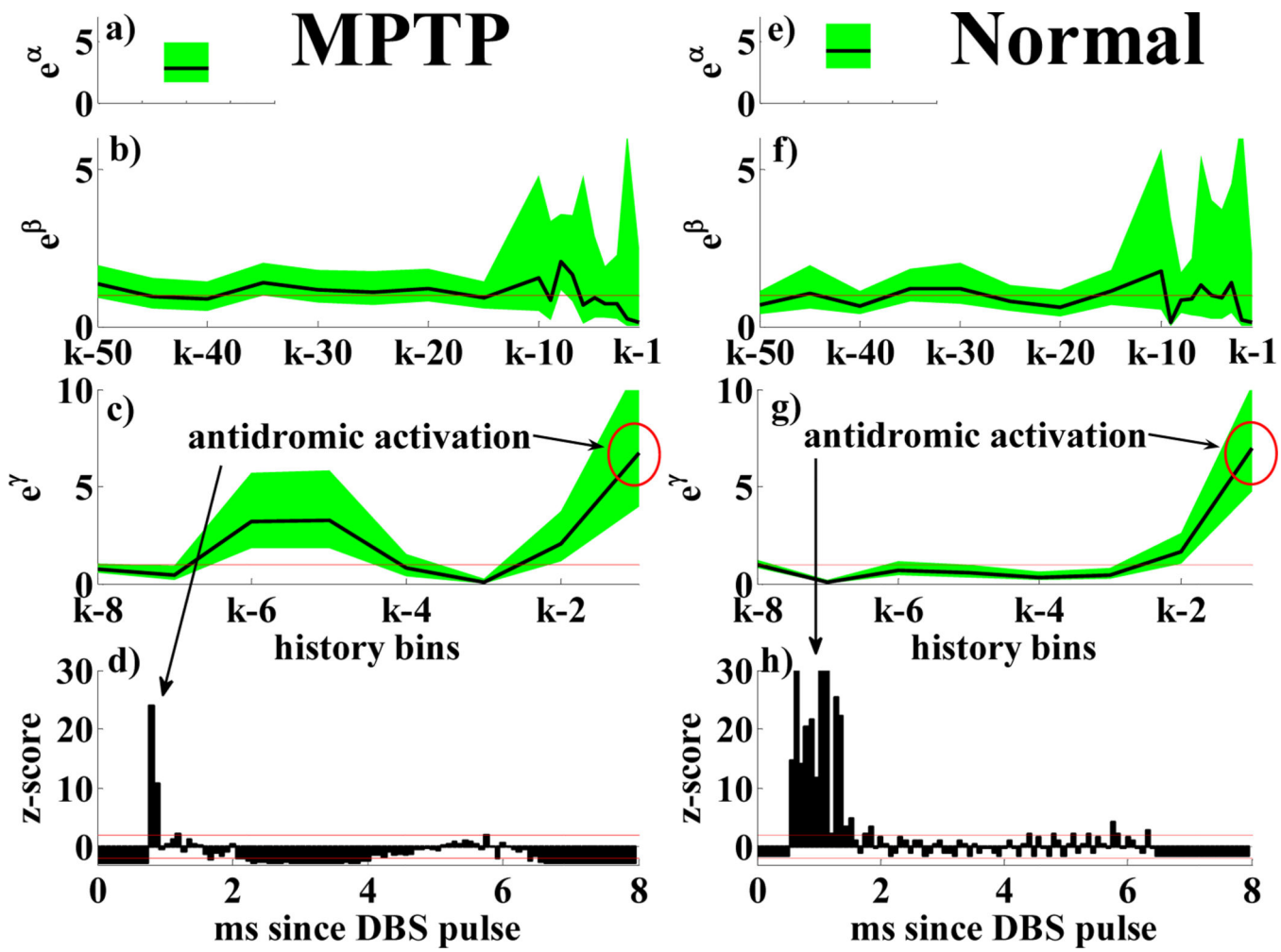

Fig. 4.

PPM for a MPTP (a–d) and normal (e–h) neuron with 130 Hz DBS. Details as in Fig. 3. PSTH in h) truncated on top.

TABLE I

Experimental Set Up (No. of Neurons Included)

Frequency	MPTP	Normal
no stimulation	14	75
50 Hz	3	29
100 Hz	not available	33
130 Hz	4	6

TABLE II

MPTP vs. Normal (No DBS)

	MPTP	Normal
Discharge frequency (Hz)	8.23±0.11	10.9±0.06
Neurons with refractoriness	6/14	23/75
Neurons with bursting (3–7 ms)	10/14	11/75
Neurons with oscillations (20–30 Hz)	11/14	17/75
Dependency from ensemble (3–7 ms)	30/51	62/241
Dependency from ensemble (10–30 ms)	24/51	41/241

TABLE III

50 vs. 100 Hz DBS (Normal)

	50 Hz	**100 Hz**
Discharge frequency (Hz)	10.9±0.20	11.0±0.18
Neurons excited 1–2 ms after pulse	2/29	1/33
Neurons excited 3–5 ms after pulse	19/29	31/33
Neurons excited 7–8 ms after pulse	13/29	33/33

TABLE IV

MPTP vs. Normal (130 Hz DBS)

	MPTP	Normal
Discharge frequency (Hz)	7.57±0.19	7.75±0.19
Neurons excited 1–2 ms after pulse	3/4	4/6
Neurons excited 3–5 ms after pulse	2/4	4/6
Neurons excited 7–8 ms after pulse	0/4	0/6